JACS
ARTICLES

A Novel Layer-by-Layer Approach to Immobilization of Polymers and Nanoclusters

Eugene W. L. Chan, Dong-Chan Lee, Man-Kit Ng, Guohui Wu, Ka Yee C. Lee, and Luping Yu*

Contribution from the Department of Chemistry and The James Franck Institute,
The University of Chicago, 5735 South Ellis Avenue, Chicago, Illinois 60637

Received March 11, 2002

Abstract: This paper reports a simple method for the multilayer immobilization of conjugated polymers, gold nanoparticles on solid supports. Poly(phenyenevinylene) functionalized with aldehyde and aminooxy groups was chemoselectively immobilized onto both glass and gold substrates via layer-by-layer deposition. The physical properties of the thin films were characterized by grazing angle IR, TM-AFM, fluorescence, and UV−visible spectroscopy. This methodology was also successfully applied to prepare polymer/gold nanocluster alternating multilayers. The results show that this methodology provides a general route for preparing robust and functionalizable multilayer films on solid substrates with molecular-level thickness control.

Introduction

Surface immobilization of organic polymers on solid supports to prepare nanostructured thin films has tremendous potential applications in the areas ranging from light-emitting diode to the coating for biomedical devices.[1] Thin-film fabrication approaches, including spin-coating, Langmuir−Blodgett techniques, electrostatic adsorption of oppositely charged polyelectrolytes, and covalent attachment of polymers using conventional coupling chemistry, have been previously demonstrated to produce complex multilayer structures.[2] The general utility of these methods was further broadened when quantum dots and nanoparticles were being incorporated into the polymer matrix.[3] The versatility and complexity of these polymeric composites provide new opportunities in the semiconductor, photovoltaic, and molecular electronic fields.[4] A number of reports in recent literature, for example, have made nanoparticle composite thin-film materials using layer-by-layer deposition of oppositely charged polyelectrolytes.[5] However, despite the ease of preparation, the stability of these multilayer films depends on a number of chemical factors such as polyelectrolyte concentration, pH, and hydrogen bonding.[6] Furthermore, the lack of specificity of the polymer side chains makes the coupling of multiple functional groups onto the polymer surface difficult. New strategies for fabricating generally functionalizable and chemically stable polymer films with well-defined thickness and surface functionality would be very valuable for the preparation of novel materials. In this paper, we introduce an efficient and effective methodology for the preparation of these thin films based only on the selective coupling of the reactive groups on the polymer side chains. This approach simultaneously permits covalent cross-linking of the polymer interlayer and chemical modification of the polymer surface. The approach is based on the layer-by-layer reaction between carbonyl compounds (ketones and aldehydes) and alkyloxyamine, so-called chemoselective ligation.[7−12] As a demonstration of the general utility of this methodology, we further apply this layer-by-layer reaction to

---

* To whom correspondence should be addressed. E-mail: lupingyu@midway.uchicago.edu.

(1) (a) Friend, R. H.; Gymer, R. W.; Holmes, A. B.; Burroughes, J. H.; Marks, R. N.; Taliani, C.; Bradley, D. D. C.; Dos Santos, D. A.; Bredas, J. L.; Logdlund, M.; Salaneck, W. R. *Nature* **1999**, *397*, 121. (b) Hubbell, J. A. *Biotechnology* **1995**, *13*, 565.

(2) (a) Picart, C.; Lavalle, P. H.; Hubert, P.; Cuisinier, F. J. G.; Decher, G.; Schaaf, P.; Voegel, J. C. *Langmuir* **2001**, *17*, 7414. (b) Wu, Z.; Wu, S.; Liang, Y. *Langmuir* **2001**, *17*, 7267. (c) Decher, G. *Science* **1997**, *277*, 1232. (d) Yoo, D.; Shiratori, S. S.; Rubner, M. F. *Macromolecules* **1998**, *31*, 4309. (e) Beyer, D.; Bohanon, T. M.; Knoll, W.; Ringsdorf, H. *Langmuir* **1996**, *12*, 2514. (f) Zhao, M.; Liu, Y.; Crooks, R. M.; Bergbreiter, D. E. *J. Am. Chem. Soc.* **1999**, *121*, 923.

(3) (a) Mamedov, A. A.; Belov, A.; Giersig, M.; Mamedova, N. N.; Kotov, N. A. *J. Am. Chem. Soc.* **2001**, *123*, 7738. (b) Malynych, S.; Luzinov, I.; Chymanov, G. *J. Phys. Chem. B* **2002**, *106*, 1280.

(4) *Nanoparticles and Nanostructured Films*; Fendler, J. H., Ed.; Wiley-VCH: Weinheim, 1998.

(5) (a) Westenhoff, S.; Kotov, N. A. *J. Am. Chem. Soc.* **2002**, *124*, 2448. (b) Hicks, J. F.; Seok-Shon, Y.; Murray, R. W. *Langmuir* **2002**, *18*, 2288. (c) Wang, T. C.; Rubner, M. F.; Cohen, R. E. *Langmuir* **2002**, *18*, 3370. (d) Gittins, D. I.; Caruso, F. *J. Phys. Chem. B* **2001**, *105*, 6846. (e) Sun, S.; Anders, A.; Hamann, H. F.; Thiele, J.-U.; Baglin, J. E. E.; Thomson, T.; Fullerton, E. E.; Murray, C. B.; Terris, B. D. *J. Am. Chem. Soc.* **2002**, *124*, 2884. (f) Ostrander, J. W.; Mamedov, A. A.; Kotov, N. A. *J. Am. Chem. Soc.* **2001**, *123*, 1101. (g) Mamedov, A. A.; Belov, A.; Giersig, M.; Mamedova, N. N.; Kotov, N. A. *J. Am. Chem. Soc.* **2001**, *123*, 7738. (h) Cassagneau, T.; Mallouk, T. E.; Fendler, J. H. *J. Am. Chem. Soc.* **1998**, *120*, 7848. (i) Fendler, J. H. *Chem. Mater.* **1996**, *8*, 1616.

(6) (a) Dubas, S. T.; Schlenoff, J. B. *Macromolecules* **2001**, *34*, 3736. (b) Shiratori, S. S.; Rubner, M. F. *Macromolecules* **2000**, *33*, 4213. (c) Clark, S. L.; Hammond, P. T. *Langmuir* **2000**, *16*, 10206.

(7) (a) Schnolzer, M.; Kent, S. B. H. *Science* **1992**, *256*, 221. (b) Lemieux, G. A.; Bertozzi, C. R. *Trends Biotechnol.* **1998**, *16*, 506.

(8) (a) Dawson, P. E.; Muir, T. W.; Clark-Lewis, I.; Kent, S. B. H. *Science* **1994**, *266*, 776. (b) Lu, W.; Qasim, M. A.; Kent, S. B. H. *J. Am. Chem. Soc.* **1996**, *118*, 8518. (c) Canne, L. E.; Bark, S. J.; Kent, S. B. H. *J. Am. Chem. Soc.* **1996**, *118*, 5891. (d) Zhang, L.; Tam, J. P. *J. Am. Chem. Soc.* **1997**, *119*, 2363.

(9) Canne, E. L.; Ferre-D'Amare, A. R.; Burley, S. K.; Kent, S. B. H. *J. Am. Chem. Soc.* **1995**, *117*, 2998.

(10) Lemieux, G. A.; Bertozzi, C. R. *Trends Biotechnol.* **1998**, *16*, 506.

(11) (a) Rose, K. *J. Am. Chem. Soc.* **1994**, *116*, 30. (b) Rose, K.; Zeng, W.; Regamey, P.-O.; Chernushevich, I. V.; Standing, K. G.; Gaertner, H. F. *Bioconjugate Chem.* **1996**, *7*, 552.

(12) Ni, Q.; Yu, L. P. *J. Am. Chem. Soc.* **1998**, *120*, 1645.

10.1021/ja026159o CCC: $22.00

immobilize monolayer protected gold nanoparticles into the interlayers of the polymeric multilayer films.

Our interest in using chemoselective ligation as a method for immobilizing polymers is initially motivated by its general utility in the selective coupling of peptides and proteins in biological systems.[7−11] This utility derives from the fact that the two chemoselective partners will react predominantly with each other, even in the presence of a number of potentially reactive functional groups. Chemoselective ligation occurs rapidly under mild conditions permitting the deposition of multilayer thin films within a reasonable time frame, even in an aqueous medium. Because of the mutually exclusive reactivity of the two groups, protecting-group manipulations are typically unnecessary in the coupling reaction. For example, we have used chemoselective ligation to immobilize ketone decorated gold nanoparticles onto aminooxy terminated self-assembled monolayer on gold substrates in our previous work.[13] We found that the nanoparticles were covalently bound to the monolayer by forming a chemically stable oxime bond. Because both aldehyde and aminooxy groups can be easily introduced into most polymers, it would be straightforward to extend this coupling chemistry for immobilizing polymers onto solid supports.

Experimental Section

Preparation of Multilayers. Glass substrates derivatized with aldehyde groups (ArrayIt, CA) were immersed in a methylene chloride solution of the aminooxy-substituted poly(phenyenevinylene) (PPV) (2 mg/mL) for 4 h at room temperature before rinsing with methylene chloride. The film was then put in a methylene chloride bath and sonicated for 5 min before drying with nitrogen. The film was subsequently immersed into a solution of aldehyde-substituted PPV (2 mg/mL) for 4 h at room temperature to form the second polymer layer. Repetition of alternative dipping in aminooxy and aldehyde derivatized PPV gives the corresponding multilayer films. To fabricate polymer/gold nanoparticle multilayers, the same procedure was employed except for using chloroform as a solvent and 1 h of dipping time. A later study on the kinetics of film deposition revealed that 5 min of dipping time was sufficient to build up one polymer layer.

Instrumentation. ^{1}H NMR spectra were recorded on a Bruker AM 400 or AM 500 spectrometer. Molecular weights and distributions of polymers were determined by using gel permeation chromatography (GPC) with a Waters Associates liquid chromatograph equipped with a Waters 510 HPLC pump, Waters 410 differential refractometer, and Waters 486 tunable absorbance detector. THF was used as the eluent, and polystyrene was used as the standard. UV−vis spectra were collected by using a Shimadzu UV-2401PC recording spectrophotometer. Emission spectra were collected by using a Shimadzu RF-5301PC spectrofluorophotometer. The transmission FT-IR spectra were obtained with a Nicolet Nexus 670 FT-IR spectrometer. The transmitted signal was averaged for 32 scans at 4 cm^{-1} resolution. The grazing angle reflectance-Fourier transform infrared spectroscopy experiments were performed with a Nicolet Magna-IR 560 Fourier transform infrared spectrometer fitted with an 85° grazing angle reflectance accessory (SpectraTech) and an internal Mercury Cadmium Tellurite (MCT) detector. The reflectance signal was averaged for 10 000 scans at 4 cm^{-1} resolution. The tapping mode AFM imaging of the sample was performed in air with a Multimode Nanoscope IIIA Scanning Probe Microscope (MMAFM, Digital Instruments). Cantilevers with Olympus Tapping Mode Etched Silicon Probe (Digital Instruments), with a nominal spring constant of 42 N/m, were used in the tapping mode with a type J scanner. The drive frequency was 270−300 kHz, and the drive amplitude was between 0.9 and 1.1 V, which corresponds to 12−20 nm. The setpoint was usually around 0.75−0.81 of the free amplitude in our experiments. The pictures shown are height mode with a frame rate of 512.

Scheme 1. Synthesis of Polymers

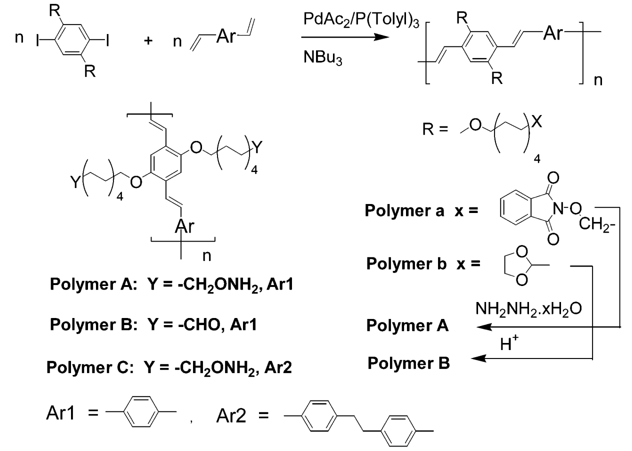

Results and Discussion

Polymer Synthesis and Characterization. To immobilize polymers onto the surface, we need polymers with complementary functional groups for chemoselective ligation. For this work, we selected to immobilize poly(phenylenevinylene) (PPV) onto solid substrates on the basis of the following reasons: (1) these are conjugated polymers exhibiting interesting physical and optical properties,[14,15] and it will be interesting to prepare multilayer films with well-controlled thickness, (2) these polymers have rigid backbones that will help to avoid complication in reaction on surface caused by the coiled chain conformation,[16] and (3) these polymers can be synthesized with a palladium-mediated Heck coupling reaction that can tolerate the corresponding functional group.[17] Scheme 1 outlines the general approach to the syntheses of both aminooxy- and aldehyde-substituted PPVs and nonconjugated PPV.

In this study, 1,4-diiodo-2,5-dialkoxybenzene was copolymerized with either 1,4-divinylbenzene or 1,2-bis(4-vinylphenyl)ethane under the standard Heck reaction condition. Toluene was used as the solvent, and the catalyst system was composed of palladium acetate (3 mol %), tributylamine (3 equiv), and tri-*o*-tolylphosphine (12 mol %). The polymerization proceeded

---

(13) Chan, E. W. L.; Yu, L. P. *Langmuir* **2001**, *17*, 311.

(14) (a) Bao, Z.; Chen, Y.; Cai, R.; Yu, L. *Macromolecules* **1993**, *26*, 5218. (b) Wang, H.; Wang, H. H.; Urban, V. S.; Littrell, K. C.; Thiyagarajan, P.; Yu, L. *J. Am. Chem. Soc.* **2000**, *122*, 6855.

(15) (a) *Handbook of Organic Conductive Molecules and Polymers*; Nalwa, H. S., Ed.; Wiley: New York, 1997. (b) Brabec, C. J.; Sariciftci, N. S.; Hummelen, J. C. *Adv. Funct. Mater.* **2001**, *11*, 15. (c) Ho, P. K. H.; Kim, J.-S.; Burroughes, J. H.; Becker, H.; Li, S. F. Y.; Brown, T. M.; Cacialli, F.; Friend, R. H. *Nature* **2000**, *404*, 481. (d) Ho, P. K. H.; Thomas, D. S.; Friend, R. H.; Tessler, N. *Science* **1999**, *285*, 233. (e) Köhler, A.; dos Santos, D. A.; Beljonne, D.; Shuai, Z.; Brédas, J.-L.; Holmes, A. B.; Kraus, A.; Müllen, K.; Friend, R. H. *Nature* **1998**, *392*, 903. (f) Granström, M.; Petritsch, K.; Arias, A. C.; Lux, A.; Andersson, M. R.; Friend, R. H. *Nature* **1998**, *395*, 257. (g) Hong, H. P.; Steitz, R.; Kirstein, S.; Davidov, D. *Adv. Mater.* **1998**, *10*, 1104. (h) Chen, L. C.; Nguyen, T. P.; Wang, X.; Sun, M. *Synth. Met.* **1998**, *94*, 239. (i) Goodson, T., III; Li, W.; Gharavi, A.; Yu, L. *Adv. Mater.* **1997**, *9*, 639. (j) Gustafsson, G.; Cao, Y.; Treacy, G. M.; Klavetter, F.; Colaneri, N.; Heeger, A. J. *Nature* **1992**, *357*, 477. (k) Burn, P. L.; Kraft, A.; Baigent, D. R.; Bradley, D. D. C.; Brown, A. R.; Friend, R. H.; Gymer, R. W.; Holmes, A. B.; Jackson, R. W. *J. Am. Chem. Soc.* **1993**, *115*, 10117.

(16) (a) Park, S. Y.; Barrett, C. J.; Rubner, M. F.; Mayes, A. M. *Macromolecules* **2001**, *34*, 3384. (b) Shiratori, S. S.; Rubner, M. F. *Macromolecules* **2000**, *33*, 4213. (c) Yoo, D.; Shiratori, S.; Rubner, M. F. *Macromolecules* **1998**, *31*, 4309.

(17) Peng, Z.; Yu, L. P. *J. Am. Chem. Soc.* **1996**, *118*, 3777.

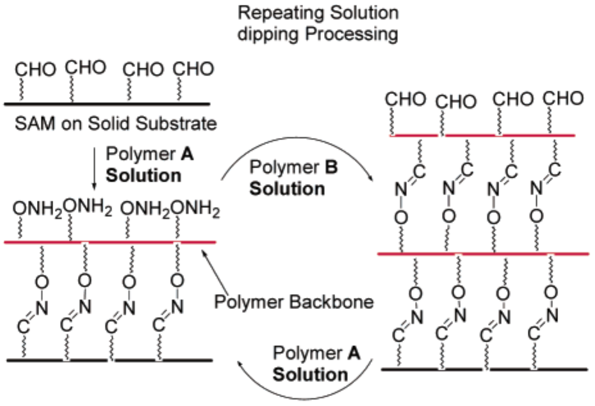

Figure 1. Multilayer deposition of PPV onto aldehyde derivatized glass substrate via chemoselective ligation.

smoothly, resulting in polymers with protected oxyamine and aldehyde moieties in high yield. Removal of the protecting groups gave the final polymers **A**, **B**, and **C** with molecular weights around Mw = 8700, 9000, and 6700 (GPC results against polystyrene standards), respectively.

The structures of the polymers were characterized by different spectroscopic techniques. The ^{1}H NMR spectra of these polymers generally feature the chemical shifts of the dialky-substituted PPV backbone. For example, the chemical shifts at 7.5 and 7.3 ppm correspond to the aromatic protons on the phenyl ring. The chemical shifts due to the vinyl protons appear around 7.1 ppm. The remaining peaks in the range of 0.9−2.7 ppm correspond to the alkyl side chains. The protons from the aldeyde and the methylene group next to the oxyamine are at 9.8 and 3.8 ppm, respectively.

Typical UV−vis absorption due to the $\pi - \pi^*$ transition of the polymer backbone was observed at $\lambda_{\max} \approx 440$ nm. Excitation at 430 nm resulted in emission spectra of these polymers at $\lambda_{\max} \approx 518$ nm. In the case of polymer **C**, blue-shifted $\lambda_{\max}$ to about 381 nm was observed due to a limited conjugation in the backbone.

Fabrication of PPV Multilayers. Figure 1 illustrates the multilayer deposition of PPV onto aldehyde derivatized glass substrates via chemoselective ligation. PPV functionalized with *n*-alkyl aminooxy side chains first reacted with the aldehyde groups on the surface to form a single layer of polymer. Subsequently, PPV derivatized with *n*-alkyl aldehyde side chains reacted with the immobilized aminooxy groups of the polymer surface to give the second layer. Repeated deposition of aminooxy and aldehyde derivatized PPV gives the corresponding multilayer films. To characterize the successive immobilization of the polymer layers on the surface, the absorption band of PPV at 440 nm was monitored by using transmission UV−vis spectroscopy (Figure 2). The linear increase in the peak absorbance with the number of layers indicates a regular deposition of the film onto the glass substrates, Figure 2 (inset).

To further demonstrate that the surface of the multilayer films possesses functional groups from the top layer, which can be used to immobilize other chemical species, rhodamine isothiocyanate was introduced to react with aminooxy groups on the film. It has been shown that PPV exhibits energy transfer behavior when a fluorescent dye is covalently bound to the polymer.[18] Figure 3 shows a fluorescence spectrum of the PPV multilayer film before and after immobilization of the dye.

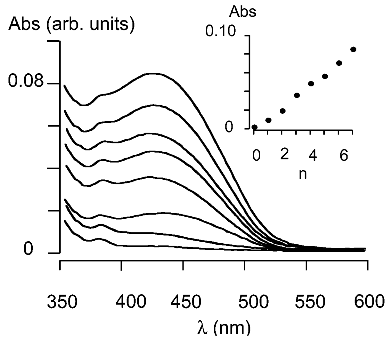

Figure 2. UV-vis absorption spectrum of multilayer of PPV immobilized onto glass substrate. The inset is a plot of the $\lambda_{\max}$ versus the number of layers.

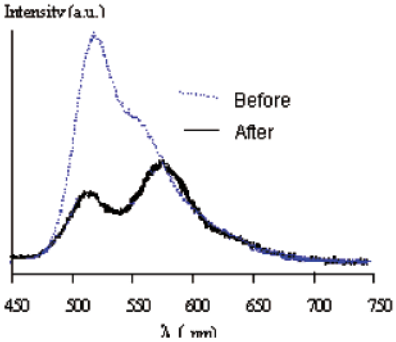

Figure 3. Fluorescence spectra of PPV multilayer film before and after immobilization of rhodamine dye.

Excitation at 430 nm gives a fluorescence emission of PPV at 520 nm. The intensity of this emission band increases with the number of layers. When rhodamine isothiocynate is coupled to the aminooxy groups of the immobilized polymer, excitation at 430 nm gives rise to an emission band at 578 nm corresponding to that of rhodamine, while the emission band for the PPV decreases in intensity. However, no dye was observed on the substrate when the polymer film was first treated with acetone prior to the immobilization of the dye. These data suggest that the surface of the multilayer film has been chemically modified by the rhodamine and that the fluorescence emission of the polymer has been partially quenched by the dye as a result. This result has two important implications. First, the surface functional groups of multilayered polymer films are reactive and can be used to immobilize a wide range of species, such as bioactive species. Second, the PPV multilayer-dye thin films may be useful as electrooptical materials, such as light-harvesting and light-emitting diodes.

Grazing angle infrared (IR) spectroscopy was used to probe the chemical modification of the polymer film. To study the multilayer film by infrared spectroscopy, the polymer was immobilized onto aminooxy terminated self-assembled monolayers (SAMs) on gold. Figure 4 shows a grazing angle IR of the multilayer deposition of PPV onto the monolayer.

When PPV-aldehyde was first immobilized onto aminooxy terminated SAMs, two peaks at 1740 and 1653 cm^{-1} corresponding to the aldehyde and oxime, respectively, appeared. After a second layer of PPV-hydroxyamine was deposited onto the substrate, the peak at 1740 cm^{-1} disappeared, while the peak at 1653 cm^{-1} increased in intensity. This clearly shows that

---

(18) Richter, B.; Kirstein, S. *J. Chem. Phys.* **1999**, *111*, 5191.

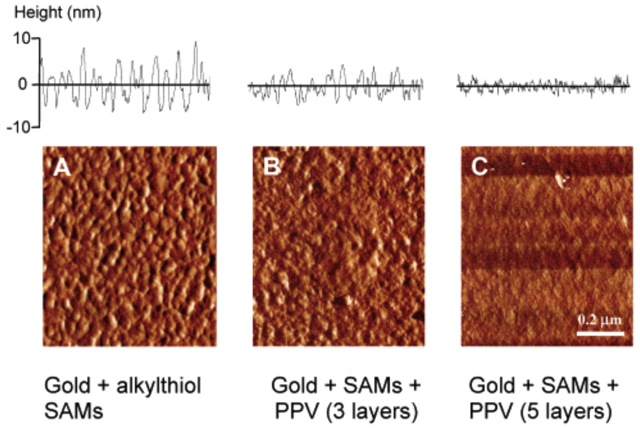

Figure 4. TM AFM images of aminooxy terminated SAMs on gold (A) after deposition of three layers (B) and five layers (C) of PPV. Line profiles of the AFM images show the relative surface roughness of the substrate.

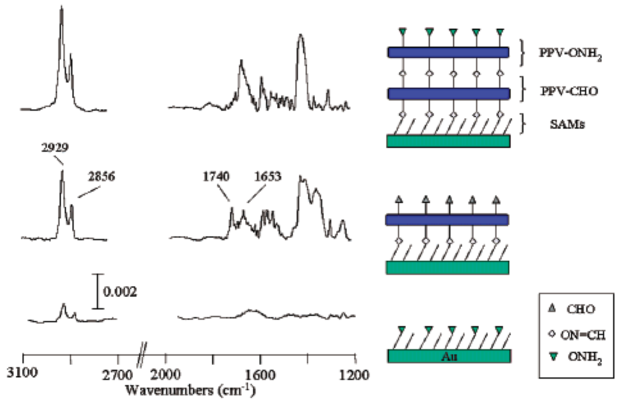

Figure 5. Grazing angle FT-IR spectra of layered polymer films.

the aminooxy group chemoselectively reacted with the aldehyde group to form a stable oxime, resulting in the immobilization of the polymers.

The surface morphology of the PPV multilayer film was examined by using tapping mode atomic force microscopy (TM AFM). Figure 5 shows TM AFM images of the gold substrate as a result of the multilayer deposition of PPV.

Prior to the immobilization of the polymer, the AFM image (Figure 5A) reveals that the surface morphology of SAMs coated gold substrate exhibits rough grained structures and appears visibly different after deposition of three layers (Figure 5B) and five layers of PPV (Figure 5C). The AFM images here showed that immobilization of the polymer films patched up the grain boundary and smoothed out the surface of the gold substrate. This result is important in preparing defect-free coating for applications in biomedical devices and electronic systems.

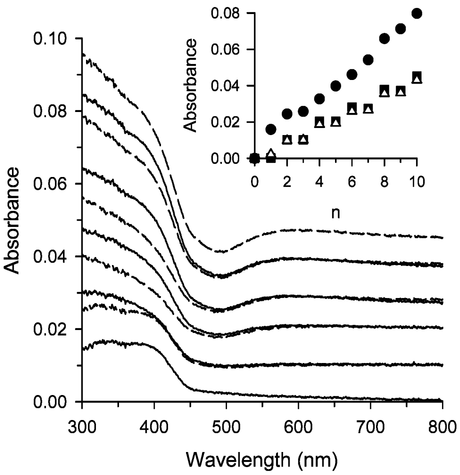

Figure 6. UV-vis absorption spectrum of the alternating multilayers of polymer **C** and gold nanoparticles immobilized onto glass substrate. The inset is a plot of the increase of absorbance at 384 (●), 516 (△), and 800 nm (■) versus the number of layers.

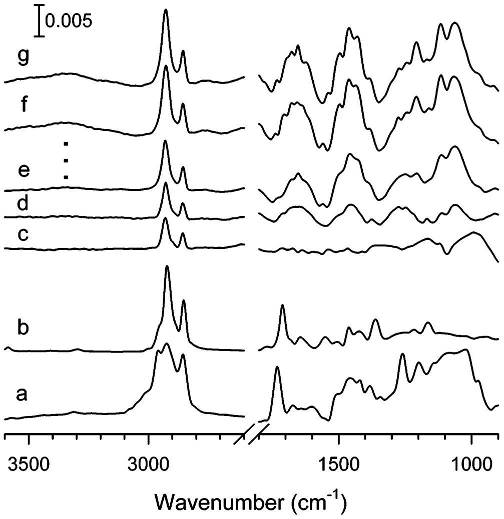

Figure 7. Transmission FT-IR spectra of polymer **C** (a) and gold nanoparticle decorated with alkyl ketonethiol (b), respectively. Spectra from c to g represent grazing angle FT-IR: c, oxyaminethiol on substrate; d, 1 layer of gold nanoparticle; e, 1/1 layers of gold nanoparticle/polymer; f, 4/3 of layers of gold nanoparticle/polymer; g, 4/4 layers of gold nanoparticle/polymer, respectively. Scales of transmission FT-IR spectra are adjusted for comparison. The scale bar is only applicable to spectra from c to g.

Fabrication of Polymer/Gold Nanoparticle Multilayers. To demonstrate the versatility of this approach, we also prepared polymer/gold nanoparticle multilayers by chemoselective ligation. The gold nanoparticles, decorated with decanethiol and alkyl ketonethiol, were prepared according to the previous procedure.[13,19] Both polymer **A** and polymer **C** can be used to prepare alternating multilayers. The alternating multilayers of polymer **C** and gold nanoparticle were fabricated by simple alternative dipping in $CHCl_3$ solution. To ensure the complete reaction, the initially employed dipping and rinsing periods were 1 h and 5 min, respectively. The multilayer deposition was monitored by increase in visible absorbance as a function of the number of layers. Figure 6 shows the increase in UV−vis absorption as a function of the number of layers. Note that the solution of polymer **C** in $CHCl_3$ has λ_{max} at 384 nm, while Au colloid has λ_{max} at 516 nm.

The deposition of the gold layer gives an increase in absorbance at 800 nm, which was absent in the colloidal state. This can be attributed to the scattering caused by the gold nanoparticle. It should be noted that the scattering increases linearly with the number of gold layers.

To ensure that the immobilization process is driven by the formation of the oxime bond after the reaction between oxyamine and ketone, the multilayers were again characterized by grazing angle FT-IR spectroscopy (Figure 7).

---

(19) Brust, M.; Walker, M.; Betherll, D.; Schiffrin, D. J.; Whyman, R. *J. Chem. Soc., Chem. Commun.* **1994**, 801. Templeton, A. C.; Wuelfing, W. P.; Murray, R. W. *Acc. Chem. Res.* **2000**, *33*, 27.

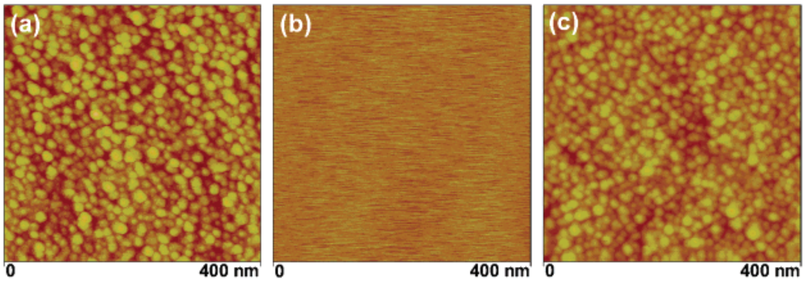

Figure 8. TM-AFM images of one layer of gold nanoparticle (a), gold nanoparticle/polymer layers (b), and gold nanoparticle/polymer/gold nanoparticle layers (c), respectively.

An oxyaminothiolate SAM on gold film on silicone wafer was used as the substrate, and gold nanoparticle and polymer layers were deposited alternatively. Similar to results shown in Figure 4, the grazing angle FT-IR spectrum (c−g) of multilayers supported the formation of oxime bonds, in comparison with the transmission FT-IR spectrum of polymer and gold nanoparticle decorated partially with ketonethiol on an NaCl IR window (a and b, respectively). The spectrum of the oxyaminethiolate SAM (c) showed only alkyl stretching bands. When the gold nanoparticle is the outmost layer (d and f), a characteristic C═O stretching band at 1715 cm^{-1} becomes more distinguishable. Deposition of the polymer layer on top of the gold nanoparticle layer diminishes the C═O stretching band and grows a new band at 1653 cm^{-1}, which corresponds to the oxime band (e and g). The residual C═O stretching band indicates that part of the ketone did not react with oxyamine to form the oxime bond. This is understandable because not all of the ketone groups in nanoparticle are accessible by oxyamine on polymer chains. Another important observation in grazing angle FT-IR spectroscopy is that the intensity of the C−O−C band at 1208 cm^{-1} increases with the number of polymer layers, consistent with the increases in the content of polymer.

To assess the surface coverage and topography of the film, the multilayers were characterized by AFM. The substrate, evaporated gold film on mica, was functionalized with oxyaminethiol in the same way described in the grazing angle FT-IR experiment. As shown in Figure 8a, the surface was fully covered by gold nanoparticle when a layer of gold nanoparticles was immobilized.

A height profile gave only a 3 nm difference between the highest and the lowest points. When the next polymer layer was deposited, a smooth surface was observed (Figure 8b), indicating that the rough surface has been entirely covered by the polymer layer. An almost identical image to Figure 8a was obtained when the next gold nanoparticle layer was immobilized (Figure 8c), suggesting that this deposition process is highly reproducible.

To have better control in the immobilization process, kinetic studies were carried out by using UV−vis spectroscopy. We found that aldehyde functionality on glass substrate is not homogeneous. To circumvent this problem, the substrates were primed with a few layers of polymer and gold nanoparticles at a dipping period of 1 h, and then each primed substrate was immersed in the polymer solutions for various dipping periods. Figure 9 summarizes the time dependency of the deposition process of the polymer layer. That the increase in absorbance at 384 nm saturates in ca. 5 min after dipping the substrate to the polymer solution indicates that the reaction took place within a short time frame. In the case of immobilizing the gold nanoparticle layer, a longer dipping period was required to obtain the same amount of absorbance as for 1 h of dipping (Figure 9).

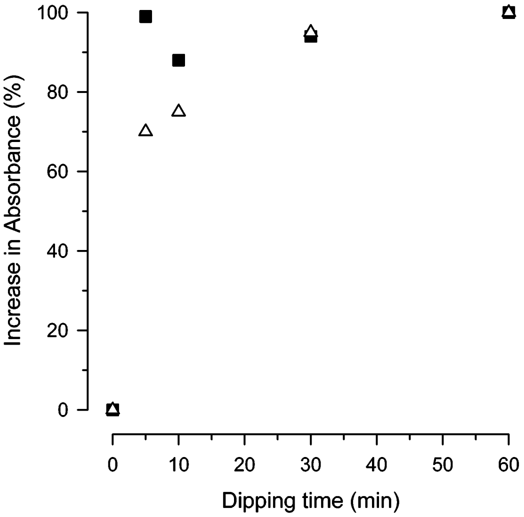

Figure 9. Plot of the absorbance at 384 (■, polymer layers) and 800 nm (△, gold nanoparticle layers) versus various dipping periods (min). Absorbance is normalized (see the text for the detailed procedure).

The kinetic difference is due to the difference in the local concentration of functional groups. When an oxyamine side group in a polymer chain reacts with ketone on the surface of the film, the neighboring oxyamine groups in the same polymer chain can have easier access to the reaction site on the surface due to close proximity, giving a zipping effect. On the other hand, during the deposition of the gold nanoparticle layer, the zipping effect cannot be observed because the ketone groups are distributed over the surface of the nanoparticles. Besides, at the end of the deposition process of the gold nanoparticle layer, the remaining space on the surface will allow only suitable sized nanoparticles. Therefore, it can be concluded that the deposition of the nanoparticle layer takes longer time to reach its saturation point than in the case of polymers.

It has been reported that inorganic nanoparticles can be deposited on a solid substrate using a polyelectrolytes-assisted layer-by-layer assembly technique, resulting in films bonded with electrostatic force.[5] Unlike reported methods, the driving force for film growth for chemoselective ligation is the formation of the covalent bond, which eventually renders great stability to the film. This approach allows one to coimmibilize the inorganic nanoparticle with various polymers in organic solvent.

Conclusions

A novel and efficient layer-by-layer polymer deposition approach was developed. The results presented here clearly show that this methodology is straightforward in fabricating robust and functionalizable polymer thin films. This approach is unique because the deposition is chemoselective and can be carried out under neutral and/or aqueous condition without adding any other reagents. The films prepared are more stable than those prepared by the polyelectrolytes approach. For example, we can treat the multilayers ultrasonically in solvents for many hours and the film is intact. The most important advantage is that the surfaces of the films are smooth in large areas ($>10\ \mu$m)[6] and contain functional groups for further attachment of other functional moieties, such as biomolecules, nanoclusters, and so on. For example, this approach permits the selective coupling of polymers and inorganic nanoparticles to solid substrates in the presence of other reactive functional groups under mild reaction conditions within a reasonable time frame. Furthermore, deposition of the polymer layers using this methodology can produce a complex multilayer structure on both glass and gold substrates with molecular-level thickness control. This methodology is well suited for studies of new polymer properties in biological systems because various polymers bearing either oxyamine or ketone groups can be synthesized. We believe this immobilization strategy will prove to be general and important for the preparation of an exciting range of tailored substrates for studies in both material science and biological application.

Acknowledgment. We gratefully acknowledge the financial supports of the National Science Foundation, AFOSR, and the NSF MRSEC program at the University of Chicago. Partial supports were also provided by UC-Argonne Nanoscience consortium and The Petroleum Research Fund, administered by the ACS.

Supporting Information Available: Synthetic procedures of polymers **A**, **B**, and **C** (PDF). This material is available free of charge via the Internet at http://pubs.acs.org.

JA026159O